



**HAL**  
open science

## Secondary organic aerosol formation from the gas-phase reaction of guaiacol (2-methoxyphenol) with NO<sub>3</sub> radicals

Lingshuo Meng, Cecile Coeur, Loyal Fayad, Nicolas Houzel, Paul Genevray, Hichem Bouzidi, Alexandre Tomas, Weidong Chen

► **To cite this version:**

Lingshuo Meng, Cecile Coeur, Loyal Fayad, Nicolas Houzel, Paul Genevray, et al.. Secondary organic aerosol formation from the gas-phase reaction of guaiacol (2-methoxyphenol) with NO<sub>3</sub> radicals. *Atmospheric Environment*, 2020, 240, pp.117740. 10.1016/j.atmosenv.2020.117740 . hal-03224419

**HAL Id: hal-03224419**

**<https://hal.science/hal-03224419>**

Submitted on 22 Aug 2022

**HAL** is a multi-disciplinary open access archive for the deposit and dissemination of scientific research documents, whether they are published or not. The documents may come from teaching and research institutions in France or abroad, or from public or private research centers.

L'archive ouverte pluridisciplinaire **HAL**, est destinée au dépôt et à la diffusion de documents scientifiques de niveau recherche, publiés ou non, émanant des établissements d'enseignement et de recherche français ou étrangers, des laboratoires publics ou privés.



Distributed under a Creative Commons Attribution - NonCommercial 4.0 International License

1 **Secondary organic aerosol formation from the gas-phase reaction of guaiacol (2-**  
2 **methoxyphenol) with NO<sub>3</sub> radicals**

3  
4 Lingshuo MENG<sup>(1,2)</sup>, Cécile COEUR<sup>(1)\*</sup>, Layal FAYAD<sup>(1)</sup>, Nicolas HOUZEL<sup>(1)</sup>, Paul  
5 GENEVRAY<sup>(3)</sup>, Hichem BOUZIDI<sup>(1)</sup>, Alexandre TOMAS<sup>(23)</sup>, Weidong CHEN<sup>(1)</sup>

6  
7 <sup>(1)</sup>Laboratoire de Physico-Chimie de l'Atmosphère, Université du Littoral Côte d'Opale,  
8 Dunkerque 59140, France

9 <sup>(2)</sup>IMT Lille Douai, Univ. Lille, SAGE – Sciences de l'Atmosphère et Génie de  
10 l'Environnement, 59000 Lille, France

11 <sup>(3)</sup>Centre Commun de Mesures, Université du Littoral Côte d'Opale, Dunkerque 59140, France

12  
13  
14 Keywords: guaiacol, NO<sub>3</sub> radicals, secondary organic aerosols, simulation chamber, nitro-  
15 aromatics.

16  
17 \*Corresponding author. Tel.: +33 328 23 76 42.

18 Address: Université du Littoral Côte d'Opale, Bâtiment IREnE, 189A, Avenue Maurice  
19 Schumann, 59140 DUNKERQUE - FRANCE

20 Email address: coeur@univ-littoral.fr (C. Coeur).

21  
22  
23  
24  
25

26 **Abstract**

27 Methoxyphenols are oxygenated aromatic compounds emitted by wood combustion  
28 (consequently to the pyrolysis of lignin). The atmospheric reaction of nitrate radical ( $\text{NO}_3$ )  
29 with guaiacol (2-methoxyphenol), one of the principal representatives of this class of  
30 compounds has been investigated in the dark at  $(294 \pm 2)$  K, atmospheric pressure and low  
31 relative humidity ( $\text{RH} < 2\%$ ). The formation of secondary organic aerosols (SOAs) has been  
32 studied in two simulation chambers. The concentrations time profiles of guaiacol were  
33 followed with a PTR-ToF-MS (Proton Transfer Mass Reaction – Time of Flight – Mass  
34 Spectrometer) and those of SOAs by an SMPS (Scanning Mobility Particle Sizer). Aerosol  
35 yields (Y) were calculated from the ratio of the suspended aerosol mass concentration  
36 corrected for wall losses ( $M_0$ ), to the total reacted guaiacol concentration assuming a particle  
37 density of  $1.4 \text{ g cm}^{-3}$ . The aerosol yield increases as the initial guaiacol concentration rises,  
38 leading to yield values ranging from 0.01 to 0.21. A very good agreement was observed  
39 between the experiments performed in both chambers which gives confidence in the data  
40 obtained in this study. The organic aerosol formation can be represented by a one-product  
41 gas/particle partitioning absorption model with a stoichiometric coefficient  $\alpha = 0.32 \pm 0.04$   
42 and an equilibrium constant  $K = (4.2 \pm 1.0) \times 10^{-3} \text{ m}^3 \mu\text{g}^{-1}$ . The chemical composition of the  
43 aerosols formed was studied after sampling on quartz fiber filter, ultrasonic extraction and  
44 analysis by ESI-LC-QToF-MS-MS (ElectroSpray Ionization - Liquid Chromatography -  
45 Quadrupole - Time of Flight – Tandem Mass Spectrometry). The oxidation products observed  
46 in the condensed phase are mostly nitro-aromatics; they display chemical structures with one,  
47 two and three aromatic rings. A reaction mechanism leading to these products has been  
48 proposed. To our knowledge, this work represents the first study on the SOAs formation from  
49 the reaction of guaiacol with  $\text{NO}_3$  radicals.

50

## 51 **1. Introduction**

52 During the last decades, air pollution has been a major issue and environmental policies have  
53 been developed to reduce its impacts on climate and air quality (Gurjar et al. 2010). Some  
54 field campaigns have shown that aromatic compounds represent about 20% of non-methane  
55 hydrocarbons in urban areas. These volatile organic compounds (VOCs) contribute to the  
56 formation of photo-oxidants (Derwent et al., 1996; Derwent et al., 1998) and Secondary  
57 Organic Aerosols (SOAs) (Calvert et al., 2002; Hallquist et al., 2009) and may involve risks  
58 for human health (Hanson et al., 1996).

59 The use of renewable energy is encouraged by environmental policies to help to decrease the  
60 dependence to fossil fuels. Biomass burning is one of the major alternative energy sources;  
61 nevertheless, it is well recognized that it also contributes to important emissions of  
62 atmospheric aerosols (Fourtziou et al., 2017), VOCs (Bruns et al., 2017) and have significant  
63 impacts on human health (Lighty et al., 2000; Sarigiannis 2015), regional and global air  
64 quality (Lelieveld et al., 2001) and climate (Chen et al., 2010; Langmann et al., 2009). Natural  
65 fires, human-initiated burning of vegetation and residential wood combustion are included in  
66 the term of “biomass burning” (Hays et al., 2002; Mazzoleni et al., 2007; McDonald et al.,  
67 2000; Schauer et al., 2001; Simpson et al., 2005).

68 The pyrolysis of lignin, one of the major components of wood, produces methoxyphenols.  
69 The principal atmospheric representatives of this class of compounds are guaiacol (2-  
70 methoxyphenol), syringol (2,6-dimethoxyphenol) and their derivatives (Hays et al., 2002;  
71 Mazzoleni et al., 2007; McDonald et al., 2000; Schauer et al., 2001; Simpson et al., 2005).  
72 They are semi-volatile compounds with high molecular weight and are distributed between  
73 gas- and particle- phases.

74 The reactivity of methoxyphenols toward hydroxyl radicals (Coeur-Tourneur et al., 2010a;  
75 Lauraguais et al., 2012, 2014a, 2015), chlorine atoms (Lauraguais et al., 2014b), ozone (El

76 Zein et al., 2015) and nitrate radicals (Lauraguais et al., 2016; Yang et al., 2016; Zang et al.,  
77 2016) has been investigated. The determination of the rate coefficients for these reactions has  
78 demonstrated their high reactivity toward OH, Cl and NO<sub>3</sub> and their low reactivity with O<sub>3</sub>.  
79 The corresponding atmospheric lifetimes are about 2 h (OH), 20 h (Cl), 1 min (NO<sub>3</sub>) and 12  
80 days (O<sub>3</sub>), respectively. Therefore, under atmospheric conditions, the main degradation  
81 pathways for the methoxyphenols are their reactions with hydroxyl radicals in the daytime  
82 and with NO<sub>3</sub> radicals, during the night.

83 The formation of secondary organic aerosols from guaiacol and syringol with respect to their  
84 reaction with OH has also been investigated (Lauraguais et al., 2012; Lauraguais et al.,  
85 2014a). In most environments, atmospheric aerosol concentrations of around 5 µg m<sup>-3</sup> can be  
86 found and in these atmospheric conditions the OH reactions of guaiacol and syringol  
87 contribute for a minor part to SOAs production.

88 The objective of this work was to study the reaction of guaiacol, a wood burning emitted  
89 compound, with NO<sub>3</sub> radicals in order to investigate its potential to form SOAs. The  
90 experiments were performed in the dark, in two simulation chambers at (294 ± 2) K,  
91 atmospheric pressure and low relative humidity (RH < 2 %). The SOA yields were measured  
92 and the data analyzed according to the absorptive gas-particle partitioning model developed  
93 by Pankow (1994a,b) and Odum et al. (1996). The oxidation products formed in the aerosols  
94 were analyzed by ESI-LC-QToF-MS-MS (ElectroSpray Ionization - Liquid Chromatography  
95 - Quadrupole - Time of Flight - Tandem Mass Spectrometry). The atmospheric implications  
96 of the reaction of guaiacol with NO<sub>3</sub> radicals were also discussed. To our knowledge, this  
97 work represents the first study on the formation of SOAs from the reaction of guaiacol with  
98 nitrate radicals.

99

## 100 **2. Materials and methods**

101 The experiments were performed in the dark in two simulation chambers, LPCA-ONE and  
102 CHARME at room temperature ( $294 \pm 2$  K), atmospheric pressure and low relative humidity  
103 ( $RH < 2\%$ ).

104 LPCA-ONE is an  $8.0 \text{ m}^3$  ( $2 \text{ m} \times 2 \text{ m} \times 2 \text{ m}$ ) PMMA (PolyMethyl Methacrylate) cubic reactor  
105 stirred by a Teflon fan (diameter 30 cm) located in the center of the lower face. A detailed  
106 description of the chamber is available in Lauraguais et al. (2012). CHARME (Chamber for  
107 the Atmospheric Reactivity and the Metrology of the Environment) is a  $9.2 \text{ m}^3$  evacuable  
108 cylinder (diameter  $\approx 1.7 \text{ m}$  and length  $\approx 4.0 \text{ m}$ ) made in stainless steel (304 L) and  
109 electropolished. Four fans (in stainless steel; diameter 50 cm) located in the bottom assure a  
110 fast homogenization of the reactive mixture.

111 Purified and dried air was introduced into both chambers using a generator (Parker Zander  
112 KA-MT 1-8) connected to a compressor (SLM-S 7.5 - Renner SCROLLLine). LPCA-ONE  
113 was flushed for a minimum of 12 h before each experiment and CHARME is coupled to a  
114 vacuum pump (Cobra NC0100-0300B), which allows to reduce the pressure down to 0.4  
115 mbar. The time required to evacuate and fill this latter reactor was around 1 h. After cleaning  
116 the chambers, satisfactory background particle number concentrations below  $10 \text{ particles cm}^{-3}$   
117 could be detected by a Scanning Mobility Particle Sizer (SMPS TSI, CPC 3775 / DMA 3081).  
118 Guaiacol was introduced into the simulation chambers using an inlet system in which  
119 measured amounts of the substances were gently heated in a small flow of purified air.

120 Nitrate radicals were generated using two methods:

121 - (i) in situ formation of  $\text{NO}_3$  from reactions (1):

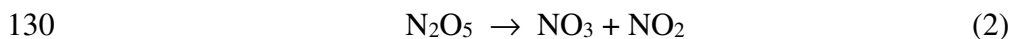


123  $\text{NO}_2$  was injected first with a gas syringe and  $\text{O}_3$  was then introduced using an ozone  
124 generator (by Corona discharge in  $\text{O}_2$ , Model C-Lasky, C-010-DTI). The injection of both  
125 gases were performed in a few seconds. The nitrogen dioxide and ozone concentrations were

126 measured with a chemiluminescence NO<sub>x</sub> analyzer (Thermo Scientific, 42i) and a photometric  
127 ozone analyzer (Thermo Scientific, 49i), respectively.

128

129 - (ii) thermal decomposition of dinitrogen pentoxide (N<sub>2</sub>O<sub>5</sub>) (Atkinson et al., 1984):



131 N<sub>2</sub>O<sub>5</sub> was first synthesized in a vacuum line through the reaction of NO<sub>2</sub> with an excess of O<sub>3</sub>  
132 according to reaction (1) followed by reaction (-2):



134 The first phase of the synthesis consisted in trapping NO<sub>2</sub> (in the form of N<sub>2</sub>O<sub>4</sub> crystals) at  
135 193 K in a cold tube. In a second phase, the tube was flushed with ozone (C-Lasky C-010-  
136 DTI) to form N<sub>2</sub>O<sub>5</sub>. Dinitrogen pentoxide crystals were gathered in a second cold trap and  
137 kept for several weeks at 188 K.

138 The experiments were performed with guaiacol initial concentrations in the range (84 - 537  
139 ppb). After allowing a few minutes for guaiacol mixing, NO<sub>2</sub> (500 - 1500 ppb) and O<sub>3</sub> (500 -  
140 1000 ppb) or N<sub>2</sub>O<sub>5</sub> were then introduced (in a few seconds) into the chambers. The  
141 concentration of guaiacol was monitored every 10 s with a Proton Transfer Reaction - Time of  
142 Flight - Mass Spectrometer (PTR-ToF-MS 1000, Ionicon Analytik GmbH). The air samples  
143 were collected through a heated (333 K) peek inlet tube with a flow of 50 mL min<sup>-1</sup> into the  
144 PTR-ToF-MS drift tube and guaiacol was monitored from the peak at m/z 125.

145 The aerosol formation was followed with a SMPS using a 2 min scan time and a 16 s delay  
146 between samples, providing a size distribution from 15 to 661 nm. The aerosol mass  
147 concentration M<sub>0</sub> was calculated assuming a density of 1.4 for the organic aerosol  
148 (recommended value, Hallquist et al., 2009).

149 Preliminary experiments were performed to verify that the guaiacol ozonolysis was negligible  
150 in the experiments where NO<sub>3</sub> was formed in-situ from NO<sub>2</sub> + O<sub>3</sub> (this was expected as the

151 rate constant for the ozone reaction with guaiacol is low ( $k_{(\text{guaiacol}+\text{O}_3)} = 4 \times 10^{-19} \text{ cm}^3 \text{ molecule}^{-1}$   
152  $\text{s}^{-1}$ , El Zein et al., 2015)).

153 Background aerosol formation could occur from the reaction of nitrate radicals with  
154 impurities in the purified air and/or with offgasing of compounds from the reactor walls. To  
155 characterize this particle formation, purified air was left in the dark in the presence of  $\text{NO}_3$  for  
156  $\approx 1$  h. These test experiments yielded aerosol mass concentrations of  $0.2 \mu\text{g m}^{-3}$ , which is  
157 negligible compared to the SOAs mass concentrations observed from the reaction of  $\text{NO}_3$  with  
158 guaiacol (between 7 and  $547 \mu\text{g m}^{-3}$ ).

159 The SOAs wall loss rates were determined by monitoring the aerosol mass concentrations  
160 over a period of  $\approx 1$  h at the end of each experiment. SOA wall losses are described by a first  
161 order law, with a dependence on the aerosol size. They were obtained from the plot of  
162  $\ln[M]_0/\ln[M]_t$  versus the time, where  $M$  is the aerosol mass concentration (in  $\mu\text{g m}^{-3}$ ) and the  
163 subscripts  $0$  and  $t$  indicate concentrations after aerosol chemical production has stopped and at  
164 a time  $t$ , respectively.

165 The decay rates estimated in this study were in the range 5 - 44 %  $\text{h}^{-1}$ . These values are within  
166 the range reported for other chamber experiments (Coeur-Tourneur et al., 2009, 2010b; Henry  
167 et al., 2008; Hurley et al., 2001; Lauraguais et al., 2012, 2014a; Takekawa et al., 2003).

168 To determine the chemical composition of SOAs, quartz fiber filters were sampled at  $7.5 \text{ L}$   
169  $\text{min}^{-1}$  during 3 h (47 mm diameter Whatman 1851-047 QMA). Before the sample collection,  
170 filters were fired at  $500 \text{ }^\circ\text{C}$  for 12 h, and were then stored in an aluminum foil below  $4^\circ\text{C}$  until  
171 analysis. For these experiments performed with higher initial concentrations of guaiacol (2  
172 ppm), SOA masses and yields were not determined because a high fraction of the particles  
173 was outside the measurement range of the SMPS.

174 The collected aerosols were analyzed by ESI-LC-QToF-MS/MS (Agilent LC 1100 - MS  
175 6540) using the negative ionization mode (proton abstraction). The chromatographic column



176 used was a ZORBAX Extend-C18 (50 mm long  $\times$  2.1 mm i.d., 1.8  $\mu$ m pore size) thermostated  
177 at 40 °C. The MS analyses allow to access the molar mass of the identified products and the  
178 MS/MS analyses, performed at three different energies (10 eV, 20 eV and 40 eV) permit to  
179 identify the functional groups of the compounds and to propose chemical structures.

180 The filters were ultrasonically extracted twice during 30 min in 5 mL of methanol. The  
181 solution was then filtered (pore sizes 0.45  $\mu$ m; PTFE Membrane, Whatman) and the volume  
182 was gently reduced to 100  $\mu$ L under a flow of gaseous nitrogen. Finally, the volume was  
183 diluted to 1 mL with ultrapure water in order to improve the separation of the compounds  
184 during the chromatographic analysis. The mobile phase used is a mixture of water (+0.1 %  
185 formic acid) and acetonitrile (+5 mM ammonium formate); the gradient varied from 90 %  
186 water / 10 % acetonitrile at the beginning of the analysis to 100 % acetonitrile at the end.

187 4-nitroguaiacol and 5-nitroguaiacol were both commercially available, so their identification  
188 was confirmed by the correlation of the LC retention times and the mass spectra recorded  
189 under the same chromatographic conditions.

190 The compounds used in this study, their manufacturer and stated purity were: guaiacol (Alpha  
191 Aesar, 98 %), 4-nitroguaiacol (Acros Organics, 97 %), 5-nitroguaiacol (TCI, 97 %), methanol  
192 (Aldrich, 99.9%), acetonitrile (VWR, > 99.9 %), water (VWR, > 99.9 %), sodium formate  
193 (VWR, > 99 %), formic acid (Acros Organics, 99 %), dioxygene (Praxair, 99.5 %) and  
194 nitrogen dioxide (Praxair, 99 %).

195

### 196 **3. Results and Discussion**

#### 197 3.1. SOA yields

198 A series of guaiacol/NO<sub>3</sub> experiments were carried out in the dark, at atmospheric pressure,  
199 room temperature (294  $\pm$  2) K and low relative humidity (< 2 %). The initial concentrations of  
200 NO<sub>2</sub> ([NO<sub>2</sub>]<sub>0</sub>), O<sub>3</sub> ([O<sub>3</sub>]<sub>0</sub>) and guaiacol ([guaiacol]<sub>0</sub>), the guaiacol reacted concentrations

201 corrected for wall losses ( $\Delta[\text{guaiacol}]$ ), the organic aerosol mass concentrations corrected for  
202 wall losses ( $M_0$ ) and the overall SOA yields ( $Y$  defined below) are summarized in Table 1.  
203 Guaiacol was totally consumed (within 15-60 min) in all experiments, so the reacted  
204 concentrations  $\Delta[\text{guaiacol}]$  correspond to  $[\text{guaiacol}]_0$ .

205 All experiments investigating SOA yields were achieved without inorganic seed aerosol and  
206 were conducted until the suspended aerosol mass (corrected for wall losses)  $M_0$  was stable.

207 Typical time profiles of guaiacol and SOA mass concentrations are presented in Fig. 1  
208 together with time-dependent aerosol size distributions (experiment guaiacol #10; initial  
209 conditions: guaiacol (276 ppb;  $1429 \mu\text{g m}^{-3}$ );  $\text{NO}_2$  (750 ppb) and  $\text{O}_3$  (500 ppb). The formation  
210 of particles started after about 45 min when almost all guaiacol has reacted. The first aerosol  
211 size distributions were centered on a few tens of nm. Then, particle number concentrations as  
212 well as SOA mass rapidly increased to reach a plateau after  $\sim 2\text{h}$  reaction time, consistent  
213 with a slower reaction rate due to the total consumption of the organic precursor. These  
214 observations suggest that the aerosol formation is due to the  $\text{NO}_3$  reaction with guaiacol as  
215 well as with its first and second (or even further) generation products. The organic aerosol  
216 yield  $Y$  was experimentally determined as the ratio of the SOA formed ( $M_0$  in  $\mu\text{g m}^{-3}$ ) to the  
217 reacted guaiacol concentration ( $\Delta[\text{guaiacol}]$  in  $\mu\text{g m}^{-3}$ ) at the end of each experiment:

$$218 \quad Y = \frac{M_0}{\Delta[\text{guaiacol}]} \quad (\text{I})$$

219 The uncertainty on the SOA yield values can be estimated at about 30%, due to statistical and  
220 possible systematic errors on  $M_0$  and  $\Delta[\text{guaiacol}]$ . The results reported in Table 1 indicate that  
221 the initial concentration of guaiacol influenced the aerosol mass concentration formed: a  
222 higher guaiacol initial concentration led to higher SOA yields. Furthermore, as the organic  
223 aerosol mass directly affects the gas/particle partitioning by acting as the medium into which  
224 oxidation products can be absorbed, higher SOA mass leads to higher SOA yields.

225 The aerosol growth curve, represented by a plot of  $M_0$  versus  $\Delta[\text{guaiacol}]$  at the end of the  
 226 experiments is shown in Fig. 2. Each experiment is represented by a single data point. The  
 227 figure displays a linear correlation ( $R^2 = 0.92$ ), with a slope of 0.25. This latter value can be  
 228 compared with the highest SOA yields determined for the reaction of guaiacol with  $\text{NO}_3$  ( $Y =$   
 229  $0.21$ ; see Table 1) and seems to represent the high-limit aerosol yield for this reaction.  
 230 Extrapolation of the data shown in Fig. 2 suggests that the SOA production would be  
 231 negligible for guaiacol reacted concentrations lower than  $\approx 550 \mu\text{g m}^{-3}$  ( $\approx 110$  ppb). This  
 232 observation is corroborated by the results obtained for the less concentrated experiments  
 233 (guaiacol #1 and guaiacol #7 with initial guaiacol concentrations of  $436 \mu\text{g m}^{-3}$  and  $604 \mu\text{g m}^{-3}$ ,  
 234 respectively) in which the aerosol mass concentrations  $M_0$  was low (around  $10 \mu\text{g m}^{-3}$ ).  
 235 A widely-used semi-empirical model based on absorptive gas-particle partitioning of semi-  
 236 volatile products (Odum et al., 1996; Pankow, 1994a,b) allows to describe the SOA yields. In  
 237 this model, the SOA yield ( $Y$ ) of a particular hydrocarbon ( $i$ ) is given by:

$$238 \quad Y = \sum_i M_0 \frac{\alpha_i K_{om,i}}{1 + K_{om,i} M_0} \quad (\text{II})$$

239 where  $\alpha_i$  is the mass-based stoichiometric coefficient of the semi-volatile product  $i$  and  $K_{om,i}$   
 240 is the gas-particle partitioning equilibrium constant. In this study, since no organic aerosol  
 241 seed was used, the total aerosol mass is equal to the mass of the SOAs formed. Eq. II can be  
 242 fitted to the guaiacol experimental data to determine the values for  $\alpha_i$  and  $K_{om,i}$  (see Fig. 3).  
 243 The simulation of  $Y$  versus  $M_0$  with the one-product model is able to satisfactorily reproduce  
 244 the experimental data ( $R^2 = 0.94$ ). The two-products model was not retained as it leads to high  
 245 uncertainties on the values of  $\alpha_i$  and  $K_{om,i}$  (sometimes more than 100% error). The fitting  
 246 parameters  $\alpha$  and  $K_{om}$  corresponding to the one-product semi-empirical model are  $0.32 \pm 0.04$   
 247 and  $(4.2 \pm 1.0) \times 10^{-3} \text{ m}^3 \mu\text{g}^{-1}$ , respectively. Many studies on SOAs yields from aromatic  
 248 compounds have reported that the aerosol yields data should be fitted assuming two

249 hypothetical products (Odum et al., 1997; Song et al., 2005). However, a number of recent  
250 works have shown that the organic aerosol yields formed in aromatic photo-oxidation systems  
251 could be well described by assuming only one hypothetical product (Coeur-Tourneur et al.,  
252 2009, 2010a; Henry et al., 2008; Lauraguais et al., 2012, 2014a; Olariu et al., 2003; Takekawa  
253 et al., 2003). Although the organic aerosol-phase is often composed of many oxidation  
254 products, the present simulation with the one-product model indicates either that one semi-  
255 volatile organic compound is the major component of the condensed phase or that the few  
256 organics present in SOAs have similar  $\alpha_i$  and  $K_{om,i}$  values. In this latter case, the obtained  
257 constants  $\alpha_i$  and  $K_{om,i}$  would not have any intrinsic physical meaning but would rather  
258 represent mean values.

259 In their study on the reaction of guaiacol with OH performed under high  $\text{NO}_x$  conditions,  
260 Lauraguais et al. (2014a) reported a gas-particle partitioning equilibrium constant  $K_{om}$  of  $(4.7$   
261  $\pm 1.2) \times 10^{-3} \text{ m}^3 \mu\text{g}^{-1}$ , which is very close to the value determined in the present study for the  
262 reaction of guaiacol with  $\text{NO}_3$ . So, it can be assumed that the products formed in the particle  
263 phase from the gas-phase oxidation of guaiacol with both oxidants have probably similar  
264 chemical compositions, including nitrate compounds. In contrast, the mass-based  
265 stoichiometric coefficient determined for the semi-volatile products formed from the reaction  
266 of guaiacol with OH ( $\alpha = 0.83$ ) is more than twice the value of  $\alpha$  obtained for the reaction  
267 with  $\text{NO}_3$ . This suggests that the reaction products from guaiacol + OH are less volatile in  
268 general compared to those from guaiacol +  $\text{NO}_3$ . This lower volatility makes them prone to go  
269 readily into the condensed phase.

270 It is interesting to compare  $\alpha$  (0.32) to the slope in Fig. 2 (0.25).  $\alpha$  represents the total amount  
271 of the semi-volatile products formed both in the gas- and aerosol- phases, whereas  $Y$   
272 corresponds to the semi-volatile products that have been formed in the particle phase only. So,

273 this suggests that about 80% of the low-volatile compounds formed in the guaiacol reaction  
274 with NO<sub>3</sub> radicals are transferred into the particle-phase.

275

### 276 3.2. SOA chemical composition

277 ESI-LC-QTOF-MS/MS analyses were performed to characterize the composition of the SOAs  
278 formed from the gas-phase reaction of NO<sub>3</sub> with guaiacol. A typical chromatogram is  
279 presented in Fig. 4. Once the molar mass of one product is determined (by LC-QTOF-MS),  
280 the corresponding peak is fragmented using three energy values (10 eV, 20 eV and 30 eV;  
281 MS/MS analysis). A higher energy value leads to a greater fragmentation of the molecules  
282 which allows to identify the functional groups and thus to assess the chemical structures of the  
283 compounds.

284 The compounds detected in the SOAs are listed in Table 2 (major compounds, relative  
285 abundance > 4 %) and Table S1 (minor compounds, relative abundance ≤ 2 %); the indicated  
286 masses correspond to the [M-H] product ions. The relative abundances (expressed in %) were  
287 calculated from the ratio of the sum of the chromatographic peak areas of the different  
288 isomers to the total chromatographic peak area of all the peaks. This approach assumes that  
289 the mass spectrometer has the same response for every detected chemical compound. The  
290 main compounds observed in the SOAs are nitrated aromatic compounds (see Table 2):  
291 nitromethoxybenzenes (m/z = 152, 2 isomers, 9.3%); nitrocatechol(s) (m/z = 154, 1 or 2  
292 isomers (the peak width suggests the presence of two isomers, but this hypothesis could not  
293 be confirmed), 18.0%); nitroguaiacols (m/z = 168, 4 isomers, 11.7%); dinitromethoxybenzene  
294 (m/z = 197, 2 isomers, 7.6%); dinitrocatechols (m/z = 199, 3 isomers, 4.7%); dinitroguaiacols  
295 (m/z = 213, 6 isomers, 9.0%); dimeric compounds formed via the association of 1  
296 nitroguaiacol and 1 nitrocatechol (m/z = 321, 12 isomers, 5.4%) or via the association of 2  
297 nitroguaiacols (m/z = 335, 5 isomers, 18.1 %), and 2 unidentified compounds (m/z = 531,

298 8.2% and  $m/z = 584$ , 4.3%). So, this confirms that the oxidation products formed in the  
299 aerosols from the reaction of  $\text{NO}_3$  radicals with guaiacol are both first and second generation  
300 products, as suggested by the data shown in Fig. 1. However, as more than  $\approx 75\%$  of the SOA  
301 mass is generated after complete depletion of guaiacol, it is highly probable that the aerosol  
302 products are formed through reactions in the gas-phase and/or in the condensed phase (in the  
303 chamber or on the filter during the sampling). Additional experiments using lower initial  
304 guaiacol concentrations would probably reduce potential reactions occurring in the condensed  
305 phase. Figures S1-S8 (see supporting information) display  $[\text{M-H}]^+$  product ions MS/MS  
306 spectra obtained at 20 eV for the major compounds identified in the SOAs ( $m/z = 152$ , Fig.  
307 S1;  $m/z = 154$ , Fig. S2;  $m/z = 168$ , Fig. S3;  $m/z = 197$ , Fig. S4;  $m/z = 199$ , Fig. S5;  $m/z =$   
308  $213$ , Fig. S6;  $m/z = 321$ , Fig. S7 and  $m/z = 335$ , Fig. S8). The different fragments allowed to  
309 propose consistent chemical structures for the oxidation products of  $\text{NO}_3 +$  guaiacol found in  
310 the particle phase.

311 The minor compounds detected in the aerosols are shown in Table S1.

312 Among the major reaction products, 4-nitroguaiacol and 5-nitroguaiacol were clearly  
313 identified by comparing their chromatographic retention times and their MS-MS spectra to  
314 those of standards commercially available. The most abundant nitroguaiacol formed in the  
315 particle phase was 4-nitroguaiacol (91.5%), in large excess compared to 5-nitroguaiacol  
316 (5.4%) and 3-nitroguaiacol and/or 6-nitroguaiacol (3.1% for both; the standards of these two  
317 isomers do not exist, so it was not possible to distinguish them).

318 The mechanism leading to the main oxidation products identified in the SOAs is proposed in  
319 Fig. 5. It has been postulated by Atkinson et al., (1992), that the  $\text{NO}_3$  radical initiated reaction  
320 of aromatic compounds may first proceed by an ipso-addition to the OH substituent which  
321 forms a six-membered transition state intermediacy. A second mechanism starts with the  
322 electrophilic addition of the nitrate radical on the aromatic ring. These two ways lead to the

323 formation of nitric acid and a phenoxy radical, which then react with NO<sub>2</sub> to produce  
324 nitroguaiacol isomers. Similarly, the formation of dinitroguaiacols and trinitroguaiacol can be  
325 explained by the reaction of nitroguaiacols with NO<sub>3</sub> and NO<sub>2</sub>.

326 The initial oxidation steps starting from guaiacol and going to nitromethoxybenzenes and  
327 nitrocatechols are not known, as indicated in Figure 5. Since the present gas-phase chemistry  
328 knowledge of aromatic compounds is not able to address these issues, we suggest that an  
329 oxidation chemistry could take place in the condensed phase and produce the observed  
330 nitromethoxybenzenes and nitrocatechols. Investigations of the liquid-phase guaiacol  
331 oxidation would be very useful to support this assumption. In their study on gas-phase  
332 reaction products of NO<sub>3</sub> + guaiacol, Yang et al. (2016) also reported the presence of  
333 nitroguaiacols (4-nitroguaiacol and 6-nitroguaiacol; 4-nitroguaiacol being the most abundant),  
334 dinitroguaiacol (4,6-dinitroguaiacol), catechol (1,2-dihydroxybenzene) and  
335 nitromethoxybenzene in the products formed from the gas-phase of NO<sub>3</sub> reaction guaiacol.  
336 They also identified catechols from the oxidation of creosol (4-methyl-guaiacol) and syringol  
337 (6-methoxy-guaiacol). The formation of catechols was reported by Zhang et al. (2016) as  
338 well, who studied the reaction of eugenol (4-allyl-guaiacol) and ethyl-guaiacol with NO<sub>3</sub>  
339 radicals. The mechanism leading to catechols from guaiacol and its derivatives was not  
340 explained in both previous articles.

341 The formation of nitrocatechols and dinitrocatechols can then result from the reaction of NO<sub>3</sub>  
342 and NO<sub>2</sub> with catechol and nitrocatechols, respectively. The compounds with high molecular  
343 masses ( $m/z > 300$ ) display 2 to 3 aromatic cycles; they can be produced from the  
344 combination of phenoxy radicals formed from nitroguaiacol(s) and/or nitrocatechol(s).

345 For the main identified products, one isomer was always more abundant than the others (the  
346 corresponding relative abundances vary from 85 % to 99 %; see table S2).

347 The oxidation products formed in the aerosols from the gas-phase reaction of guaiacol with  
348 nitrate radicals can also be compared to those identified for the reaction of guaiacol with  
349 hydroxyl radicals under high NO<sub>x</sub> conditions (Ahmad et al., 2017). The ATR-FTIR analyses  
350 performed by Ahmad et al., (2017) also reveal the presence of 4-nitroguaiacol in the SOAs.  
351 So, this observation suggests that the oxidation products generated in the particulate phase,  
352 via the oxidation of guaiacol by NO<sub>3</sub> or OH/NO<sub>x</sub> reaction, are probably similar as it has been  
353 previously postulated from the comparison of the gas-particle partitioning equilibrium  
354 constants ( $K_{om,i}$ ) obtained with both oxidants.

355

#### 356 **4. Conclusions**

357 The formation of secondary organic aerosols from the reaction of guaiacol (2-methoxyphenol)  
358 with nitrate radicals has been studied in two simulation chambers. The SOAs yields have been  
359 shown to be influenced by the initial guaiacol concentration, which leads to aerosol yields  
360 ranging from 0.01 to 0.21. A very good agreement was observed between the experiments  
361 performed in both chambers which gives confidence in the data obtained in this study. The  
362 aerosols data have been fitted with the absorptive gas-particle partitioning model developed  
363 by Pankow (1994a,b) and Odum et al. (1996) using the one-product model.

364 Aerosol organic carbon concentration is typically 5  $\mu\text{g m}^{-3}$  in many environments, though it  
365 can occasionally rise to 50  $\mu\text{g m}^{-3}$  or more in highly polluted areas. Extrapolating to a particle  
366 loading of 5  $\mu\text{g m}^{-3}$  from the yield data (Fig. 3) gives a 2% SOA yield. Based on this result,  
367 one can infer that the contribution of the reaction between guaiacol and NO<sub>3</sub> radicals to SOAs  
368 production under atmospheric conditions is probably relatively minor. However, in polluted  
369 areas this reaction can be an important source of secondary aerosols.

370 ESI-LC-QToF-MS/MS analyses were performed to characterize the chemical composition of  
371 the aerosols. Nitro-aromatics compounds were identified as the main oxidation products,



372 confirming previous studies (Yang et al., 2016; Zhang et al., 2016) on the products formed  
373 from the gas-phase reaction of NO<sub>3</sub> radicals with guaiacol derivatives.

374 A well-established tracer for primary biomass burning aerosols (BBA) is levoglucosan (1,6-  
375 anhydro-β-anhydroglucose), which originates from the pyrolysis of cellulose or  
376 hemicelluloses (Simoneit et al., 2002). Several nitro-aromatic compounds were detected in  
377 urban aerosols, and nitrocatechols as well as nitroguaiacols are recognized to be suitable  
378 tracers for secondary BBA (Iinuma et al., 2010; Kitanovsky et al., 2012). Further research  
379 efforts on the reactivity of these compounds would allow to measure their rate constants with  
380 the main oxidants and to determine the corresponding lifetimes. To our knowledge, only a  
381 few data are available in the literature concerning the atmospheric reactivity of nitro-  
382 aromatics (Bejan et al., 2007; 2015).

383

#### 384 **Acknowledgements**

385 This work was supported by the CaPPA project (Chemical and Physical Properties of the  
386 Atmosphere) funded by the French National Research Agency (ANR-11-LABX-0005-01) and  
387 the CLIMIBIO program supported by the Hauts-de-France Regional Council, the French  
388 Ministry of Higher Education and Research and the European Regional Development Fund.

389

#### 390 **References**

391 Atkinson, R., Carter, W.P.L., Plum, C.N., Winer, A.M., Pitts, J.N., 1984. Kinetics of the gas-  
392 phase reactions of NO<sub>3</sub> radicals with a series of aromatics at 296 ± 2 K. *Int. J. Chem.*  
393 16, 887-898.

394 Atkinson R., Aschmann S. M., Arey J, 1992. Reactions of hydroxyl and nitrogen trioxide  
395 radicals with phenol, cresols, and 2-nitrophenol at 296 ± 2 K. *Environ. Sci. Technol.*  
396 26, 1397-1403.

397 Ahmad, W., Coeur C., Tomas A., Fagniez T., Brubach J-B., Cuisset A., 2017. Infrared  
398 spectroscopy of secondary organic aerosol precursors and investigation of the  
399 hygroscopicity of SOA formed from the OH reaction with guaiacol and syringol.  
400 *Appl. Opt.*, 56, 116-122.

401 Bejan, J., Barnes, I., Olariu, O., Zhou, S., Wiesen, P., Bentera, T., 2007. Investigations on the  
402 gas-phase photolysis and OH radical kinetics of methyl-2-nitrophenols. *Phys. Chem.*  
403 *Chem. Phys.*, 9, 5686-5692.

404 Bejan, J., Duncianu, M., Olariu, O., Barnes, I., Seakins, P., Wiesen, P., 2015. Kinetic study of  
405 the gas-phase reactions of chlorine atoms with 2-chlorophenol, 2-nitrophenol, and four  
406 methyl-2-nitrophenol isomers. *J. Phys. Chem. A*, 2015, 20, 4735-4745.

407 Bruns E.A. , Slowik J.G., El Haddad I., Kilic D., Klein F., Dommen J., Temime-Roussel B.,  
408 Marchand N., Baltensperger U., Prévôt A.S.H. 2017. Characterization of gas-phase  
409 organics using proton transfer reaction time-of-flight mass spectrometry: fresh and  
410 aged residential wood combustion emissions. *Atmos. Chem. Phys.*, 17, 705-720.

411 Calvert, J.G., Atkinson, R., Becker, K.H., Kamens, R.M., Seinfeld, J.H., Wallington, T.J.,  
412 Yarwood, G., 2002. The mechanisms of atmospheric oxidation of aromatic  
413 hydrocarbons, Oxford University Press, New York, N.Y.

414 Chen Y., Bond T.C., 2010. Light absorption by organic carbon from wood combustion.  
415 *Atmos. Chem. Phys.* 10, 1773–1787.

416 Coeur-Tourneur, C., Tomas, A., Guilloteau, A., Henry, F., Ledoux, F., Visez, N., Riffault, V.,  
417 Wenger, J.C., Bedjanian, Y., 2009. Aerosol formation yields from the reaction of  
418 catechol with ozone. *Atmos. Environ.* 43, 2360-2365.

419 Coeur-Tourneur C., Cassez A., Wenger J.C., 2010a. Rate constants for the gas-phase reaction  
420 of hydroxyl radicals with 2-methoxyphenol (guaiacol) and related compounds, *J. Phys.*  
421 *Chem. A* 114, 11645-11650.

422 Coeur-Tourneur C., Foulon V., Laréal M., 2010b. Determination of aerosol yields from 3-  
423 methylcatechol and 4-methylcatechol ozonolysis in a simulation chamber, *Atmos.*  
424 *Environ.* 44, 852-857.

425 Derwent, R.G., Jenkin, M.E., Saunders, S., 1996. Photochemical ozone creation potentials for  
426 a large number of reactive hydrocarbons under European conditions. *Atmos. Environ.*  
427 30, 181–199.

428 Derwent, R.G., Jenkin, M.E., Saunders, S.M., Pillings, M. J., 1998. Photochemical ozone  
429 creation potentials for organic compounds in northwest Europe calculated with a  
430 master chemical mechanism. *Atmos. Environ.* 32, 2429–2441.

431 El Zein, A., Coeur, C., Obeid, E., Lauraguais, A., Fagniez, T., 2015. Reaction kinetics of  
432 catechol (1,2-Benzenediol) and guaiacol (2-Methoxyphenol) with ozone. *J. Phys.*  
433 *Chem. A* 119, 6759-6765.

434 Fourtziou L., Liakakou E., Stavroulas I., Theodosi C., Zarnpas P., Psiloglou B., Sciare J.,  
435 Maggos T., Bairachtari K., Bougiatioti A., Gerasopoulos E., Sarda-Estève R.,  
436 Bonnaire N., Mihalopoulos N. 2017. Multi-tracer approach to characterize domestic  
437 wood burning in Athens (Greece) during wintertime. *Atmos. Environ.*, 148, 89-101.

438 Gurjar B.R., Molina L.T., Ojha C.S.P. 2010. *Air Pollution: Health and Environmental*  
439 *Impacts*. CRC Press Taylor & Francis Group.

440 Hallquist M., Wenger J. C., Baltensperger U., Rudich Y., Simpson D., Claeys M., Dommen  
441 J., Donahue N. M., George C., Goldstein A. H., Hamilton J. F., Herrmann H.,  
442 Hoffmann T., Iinuma Y., Jang M., Jenkin M. E., Jimenez J. L., Kiendler-Scharr A.,  
443 Maenhaut W., McFiggans G., Mentel Th. F., Monod A., Prévôt A. S. H., Seinfeld J.  
444 H., Surratt J. D., R. Szmigielski R., Wildt J., 2009. The formation, properties and  
445 impact of secondary organic aerosol: current and emerging issues. *Atmos. Chem.*  
446 *Phys.* 9, 5155–5236.

447 Hanson D.J., 1996. Toxics release inventory report shows chemical emissions continuing to  
448 fall. Chem. Eng. News, July 15, 29-30.

449 Hays, M.D., Geron, C.D., Linna, K.J., Smith, N.D., Schauer, J. J., 2002. Speciation of gas-  
450 phase and fine particle emissions from burning of foliar fuels. Environ. Sci. Technol.  
451 36, 2281-2295.

452 Henry, F., Coeur-Tourneur, C., Ledoux, F., Tomas, A., Menu, D., 2008. Secondary organic  
453 aerosol formation from the gas phase reaction of hydroxyl radicals with m-, o- and p-  
454 cresol. Atmos. Environ. 42, 3035–3045.

455 Hurley, M.D., Sokolov, O., Wallington, T.J., Takekawa, H., Karasawa, M., Klotz, B., Barnes,  
456 I., Becker, K.H., 2001. Organic aerosol formation during the atmospheric degradation  
457 of toluene. Environ. Sci. Technol. 35, 1358–1366.

458 Iinuma, Y, Böge, O., Agräfe R., Herrmann H., 2010. Methyl-Nitrocatechols: Atmospheric  
459 tracer compounds for biomass burning secondary organic aerosols. Environ. Sci.  
460 Technol., 44, 8453-8459.

461 Kitanovsky, Z., Grgi, I., Yasmeen, F., Claeys, M., A., 2012. Development of a liquid  
462 chromatographic method based on ultraviolet-visible and electrospray ionization mass  
463 spectrometric detection for the identification of nitrocatechols and related tracers in  
464 biomass burning atmospheric organic aerosol, Rapid Commun. Mass Sp., 26, 793-804.

465 Langmann, B., Duncan, V., Textor, C., Trentmann, J., van der Werfe, G.R., 2009. Vegetation  
466 fire emissions and their impact on air pollution and climate. Atmos. Environ. 43, 107-  
467 116

468 Lauraguais, A., Coeur-Tourneur, C., Cassez, A., Seydi, A., 2012. Rate constant and secondary  
469 organic aerosol yields for the gas-phase reaction of hydroxyl radicals with syringol  
470 (2,6-dimethoxyphenol). Atmos. Environ. 55, 43-48.

471 Lauraguais, A., Bejan, I., Coeur-Tourneur, C., Cassez, A., Deboudt, K., Fourmentin, M.,  
472 Choël, M., 2014a. Atmospheric reactivity of hydroxyl radicals with guaiacol (2-  
473 methoxyphenol), a biomass burning emitted compound : secondary organic aerosol  
474 formation and gas-phase oxidation products. *J. Phys. Chem. A* 86, 155-163.

475 Lauraguais, A., Bejan, I., Barnes, I., Wiesen, P., Coeur-Tourneur, C., Cassez, A., 2014b. Rate  
476 coefficient for the gas-phase reaction of chlorine atoms with a series of methoxylated  
477 aromatic compounds. *J. Phys. Chem. A* 118, 1777-1784.

478 Lauraguais, A., Bejan, I., Barnes, I., Wiesen, P., Coeur, C., 2015. Rate coefficients for the  
479 gas-phase reaction of hydroxyl radicals with a series of methoxylated aromatic  
480 compounds. *J. Phys. Chem. A* 119, 6179-6187.

481 Lauraguais, A., El Zein, A., Coeur, C., Obeid, E., Rayez, M-T., Rayez, J-C., 2016. Rate  
482 coefficient for the gas-phase reaction of nitrate radicals with a series of  
483 methoxyphenol compounds: experimental and theoretical approaches. *J. Phys. Chem.*  
484 *A*, 120, 2691-2699 (2016).

485 Lelieveld, J., Crutzen, P.J., Ramanathan, V., Andreae, M.O., Brenninkmeijer, C.A.M.,  
486 Campos, T., Cass, G.R., Dickerson, R.R., Fischer, H., de Gouw, J.A., Hansel, A.,  
487 Jefferson, A., Kley, D., de Laat, A.T.J., Lal, S., Lawrence, M.G., Lobert, J.M., Mayol-  
488 Bracero, O.L., Mitra, A.P., Novakov, T., Oltmans, S.J., Prather, K.A., Reiner, T.,  
489 Rodhe, H., Scheeren, H.A., Sikka, D., Williams, J., 2001. The Indian ocean  
490 experiment: widespread air pollution from South and Southeast Asia. *Science* 291,  
491 1031-1036.

492 Lighty, J.S., Veranth, J.M., Sarofim, A.F., 2000. Combustion aerosols: factors governing their  
493 size and composition and implications to human health. *J. Air Waste Manag.* 50,  
494 1565-1618.

495 Mazzoleni, L.R., Zielinska, B., Moosmüller, H., 2007. Emissions of levoglucosan,  
496 methoxyphenols, and organic acids from prescribed burns, laboratory combustion of  
497 wildland fuels, and residential wood combustion. *Environ. Sci. Technol.* 41, 2115-  
498 2122.

499 McDonald, J.D., Zielinska, B., Fujita, E.M., Sagebiel, J.C., Chow, J.C., Watson, J.G., 2000.  
500 Fine particle and gaseous emission rates from residential wood combustion. *Environ.*  
501 *Sci. Technol.* 34, 2080-2091.

502 Odum, J.R., Hoffmann, T., Bowman, F.M., Collins, D., Flagan, R.C., Seinfeld, J.H., 1996.  
503 Gas/particle partitioning and secondary organic aerosol yields. *Environ. Sci. Technol.*  
504 3, 2580-2585.

505 Odum, J.R., Jungkamp, T.P.W., Griffin, R.J., Forstner, H.J.L., Flagan, R.C., Seinfeld, J.H.,  
506 1997. Aromatics, reformulated gasoline, and atmospheric organic aerosol formation.  
507 *Environ. Sci. Technol.* 31, 1890–1897.

508 Olariu, R.I., Tomas, A., Barnes, I., Wirtz, K., 2003. Atmospheric ozone degradation reaction  
509 of 1,2-dihydroxybenzene: aerosol formation study. In: *The European Photoreactor*  
510 *EUPHORE, fourth report 2001*. Ed. Institute of Physical Chemistry, Bergische  
511 Universität Wuppertal, Germany, 54–71.

512 Pankow, J.F., 1994a. An absorption model of gas/particles partitioning of organic compounds  
513 in the atmosphere. *Atmos. Environ.* 28, 185–188.

514 Pankow, J.F., 1994b. An absorption model of the gas/aerosol partitioning involved in the  
515 formation of secondary organic aerosol. *Atmos. Environ.* 28, 189–193.

516 Sarigiannis D.A., Karakitsios S.P. , Kermenidou, M.V. 2015. Health impact and monetary  
517 cost of exposure to particulate matter emitted from biomass burning in large cities.  
518 *Sci. Total Environ.*, 15, 319-330.

519 Schauer, J.J., Kleeman, M.J., Cass, G.R., Simoneit, B.R.T., 2001. Measurement of emissions  
520 from air pollution sources. 3. C<sub>1</sub>-C<sub>29</sub> organic compounds from fireplace combustion of  
521 wood. *Environ. Sci. Technol.* 35, 1716-1728.

522 Simoneit, B. R. T., 2002. Biomass burning - a review of organic tracers for smoke from  
523 incomplete combustion. *Appl. Geochem.* 17, 129-162.

524 Simpson, C.D., Paulsen, M., Dills, R.L., Liu, L.J.S., Kalman, D.A., 2005. Determination of  
525 methoxyphenols in ambient atmospheric particulate matter: tracers for wood  
526 combustion. *Environ. Sci. Technol.* 39, 631-637.

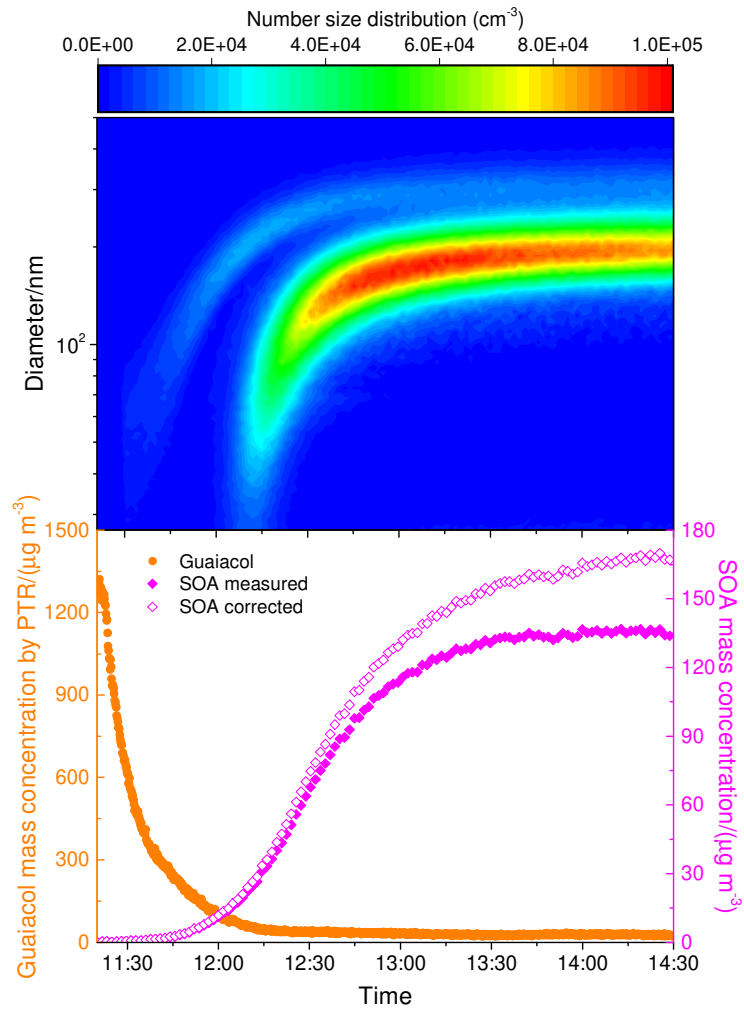
527 Song, C., Na, K., Cocker, D.R., 2005. Impact of the hydrocarbon to NO<sub>x</sub> ratio on secondary  
528 organic aerosol formation. *Environ. Sci. Technol.* 39, 3143-3149.

529 Takekawa, H., Minoura, H., Yamazaki, S., 2003. Temperature dependence of secondary  
530 organic aerosol formation by photo-oxidation of hydrocarbons. *Atmos. Environ.* 37,  
531 3413-3424.

532 Yang, B., Zhang, H., Wang, Y., Zhang P., Shu, J., Sun, W., Ma, P., 2016. Experimental and  
533 theoretical studies on gas-phase reactions of NO<sub>3</sub> radicals with three methoxyphenols:  
534 guaiacol, creosol, and syringol. *Atmos. Environ.*, 125, 243-251.

535 Zhang H., Yang, B., Wang, Y., Shu, J., Zhang, P., Ma, P., Li, Z. 2016. Gas-phase reactions of  
536 methoxyphenols with NO<sub>3</sub> radicals: kinetics, products, and mechanisms. *J. Phys.*  
537 *Chem. A*, 120, 1213-1221.

1 Fig. 1. Typical concentration-time profiles obtained for guaiacol (PTR-ToF-MS) and SOAs  
2 (SMPS; measured and corrected for wall losses). Experiment guaiacol #10 (initial mixing  
3 ratios: guaiacol (276 ppb;  $1429 \mu\text{g m}^{-3}$ );  $\text{NO}_2$  (750 ppb) and  $\text{O}_3$  (500 ppb).

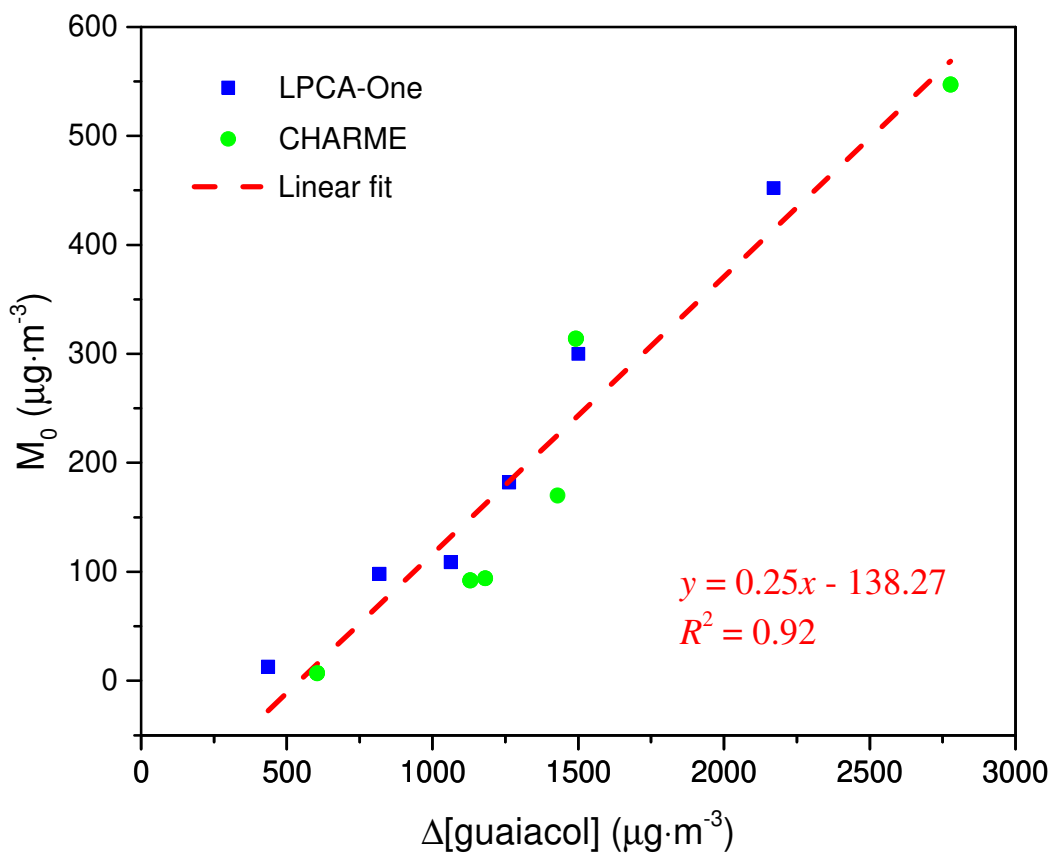


4  
5  
6



7 Fig. 2. Aerosol growth curve: SOA mass concentration ( $M_0$ ) against the reacted guaiacol  
8 concentration ( $\Delta[\text{guaiacol}]$ ) measured at the end of the experiments. Each data point  
9 represents a separate experiment.

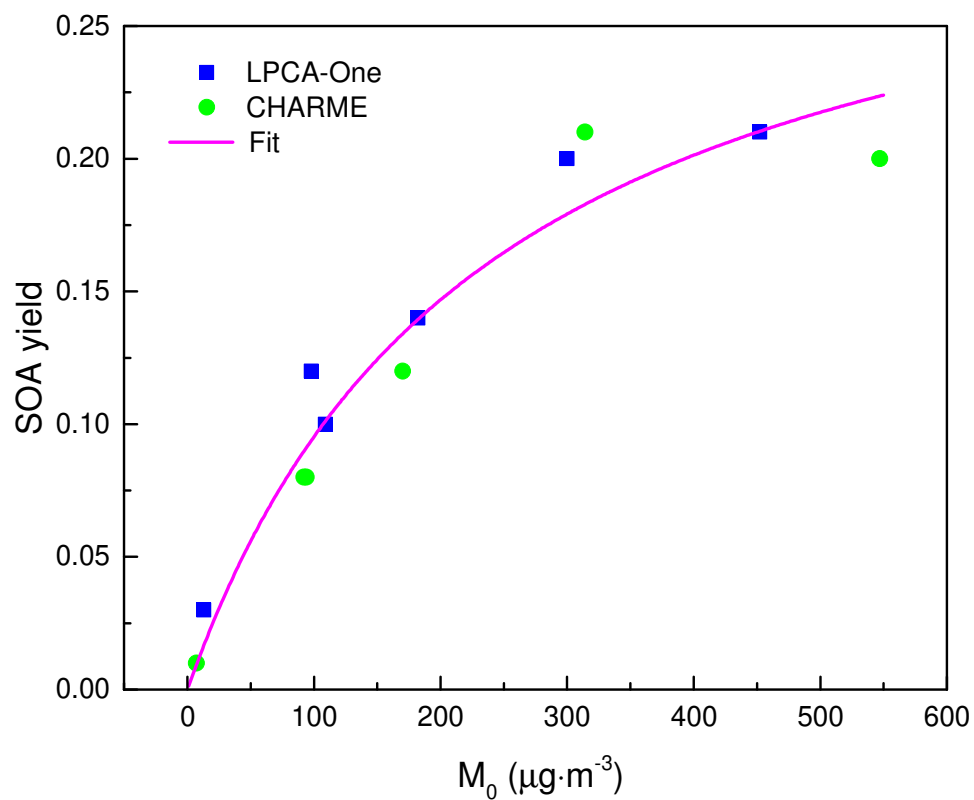
10



11

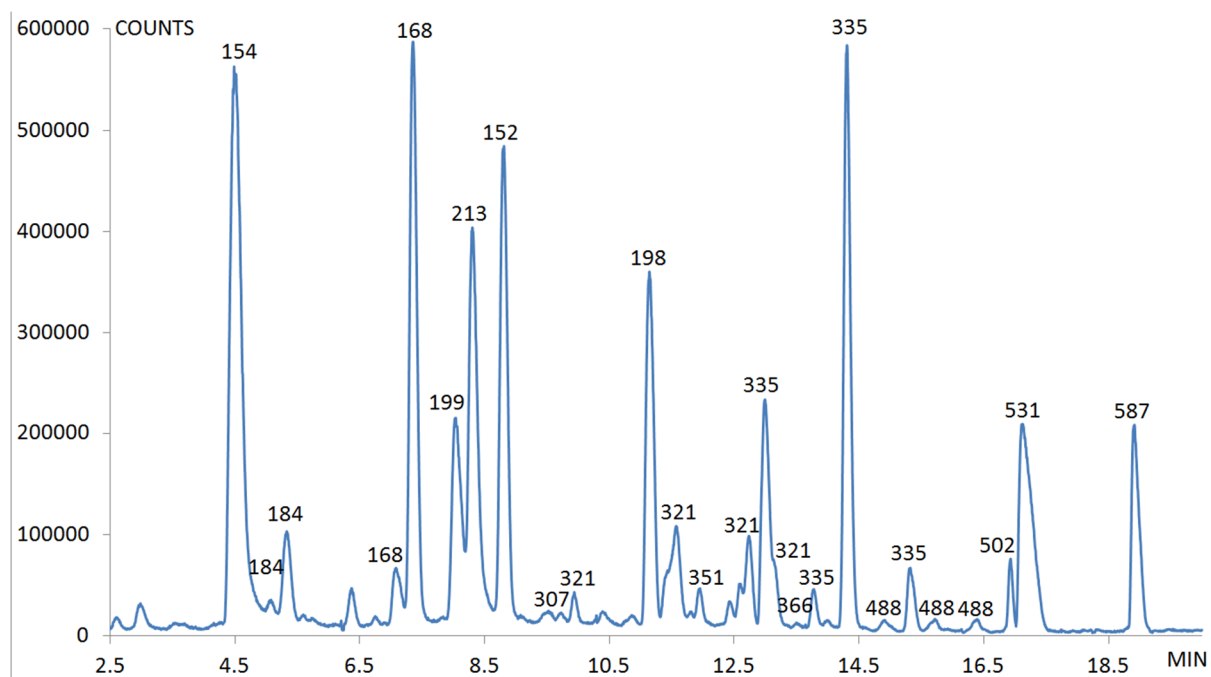
12

13 Fig. 3. Yield curve (SOA yield Y versus the organic aerosol mass formed  $M_0$ ) for  
14 guaiacol/ $\text{NO}_3$  experiments in LPCA-One (blue squares) and in CHARME (green circles). The  
15 line represents the best fit to the data considering one semi-volatile major product. The fitting  
16 parameters used are  $\alpha = 0.32 \pm 0.04$  and  $K_{\text{om}} = (4.2 \pm 1.0) \times 10^{-3} \text{ m}^3 \mu\text{g}^{-1}$ .  
17



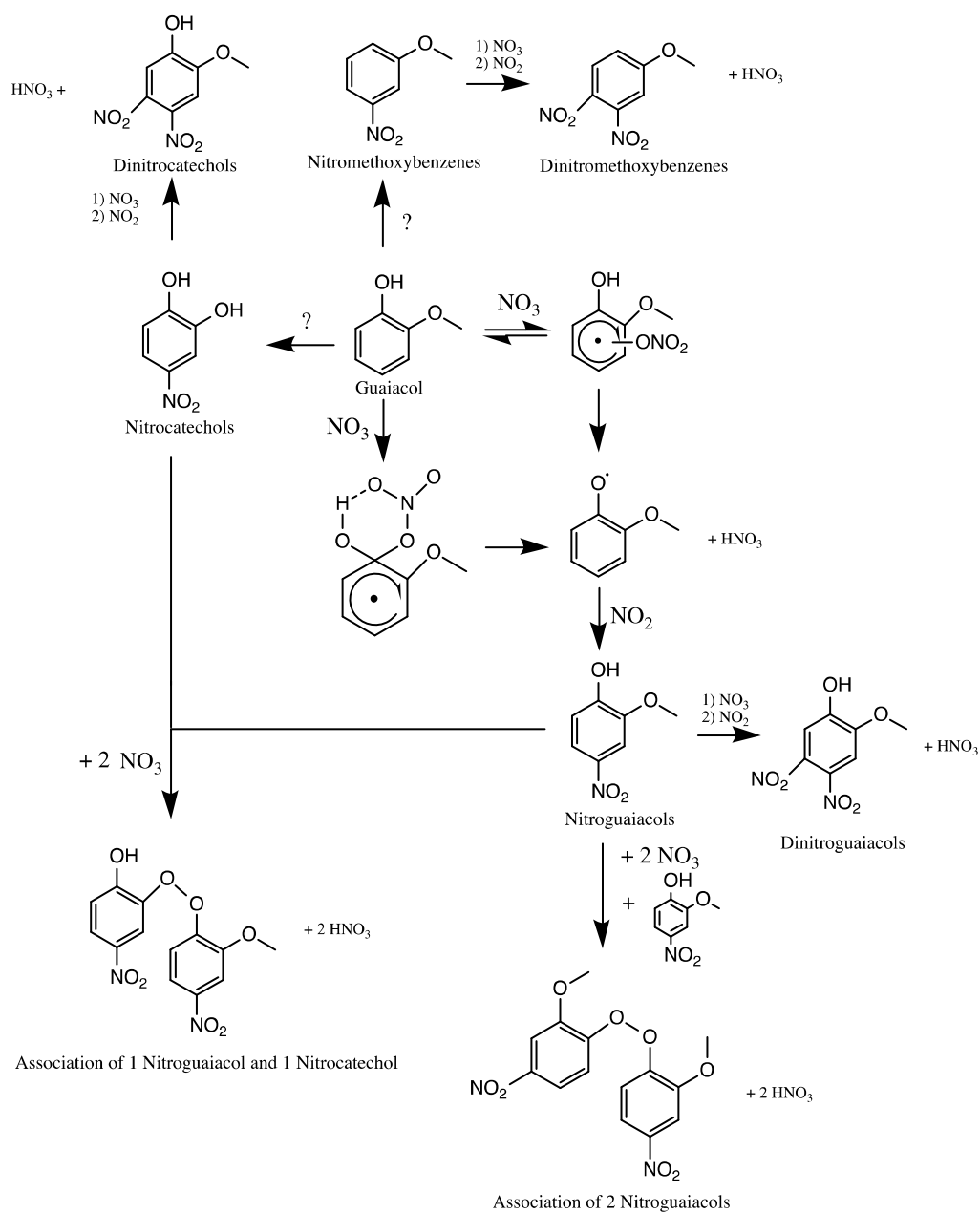
18

19 Fig. 4. Chromatogram (ESI-LC-QToF-MS/MS analysis) of the SOAs formed from the gas-  
20 phase reaction of guaiacol (2-methoxyphenol) with NO<sub>3</sub> radicals. The compounds  
21 corresponding to the labelled peaks are displayed in table 2. The indicated masses correspond  
22 to the [M-H]<sup>+</sup> product ions.



23  
24  
25

26 Fig.5. Detailed mechanism leading to the main products observed in the SOAs formed from  
 27 the gas-phase reaction of guaiacol (2-methoxyphenol) with NO<sub>3</sub> radicals.



28

1 **Table 1.** Experimental conditions and results.

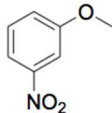
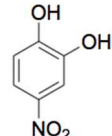
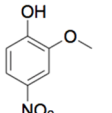
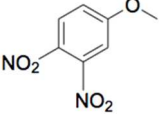
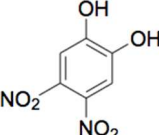
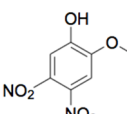
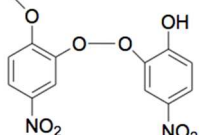
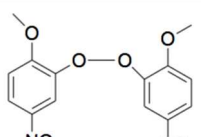
Expt.	[guaiacol] <sub>0</sub> <sup>a</sup> (ppb)	NO <sub>3</sub> formation		Δ[guaiacol] <sup>b</sup> (μg m <sup>-3</sup> )	M <sub>0</sub> <sup>c</sup> (μg m <sup>-3</sup> )	Y <sup>d</sup>
		[NO <sub>2</sub> ] <sub>0</sub>	[O <sub>3</sub> ] <sub>0</sub>			
		(ppb)	(ppb)			
<b>In LPCA-ONE</b>						
guaiacol #1	84	N <sub>2</sub> O <sub>5</sub> decomposition		436	13	0.03
guaiacol #2	158	N <sub>2</sub> O <sub>5</sub> decomposition		818	98	0.12
guaiacol #3	206	N <sub>2</sub> O <sub>5</sub> decomposition		1063	109	0.10
guaiacol #4	244	N <sub>2</sub> O <sub>5</sub> decomposition		1263	182	0.14
guaiacol #5	290	N <sub>2</sub> O <sub>5</sub> decomposition		1501	300	0.20
guaiacol #6	420	N <sub>2</sub> O <sub>5</sub> decomposition		2171	452	0.21
<b>In CHARME</b>						
guaiacol #7	117	N <sub>2</sub> O <sub>5</sub> decomposition		604	7	0.01
guaiacol #8	218	785 <sup>e</sup>	896 <sup>f</sup>	1130	92	0.08
guaiacol #9	228	535 <sup>e</sup>	620 <sup>f</sup>	1181	94	0.08
guaiacol #10	276	750 <sup>g</sup>	500 <sup>h</sup>	1429	170	0.12
guaiacol #11	288	1239 <sup>e</sup>	798 <sup>f</sup>	1492	314	0.21
guaiacol #12	537	1500 <sup>g</sup>	1000 <sup>h</sup>	2778	547	0.20

2

3 <sup>a</sup>Initial guaiacol volume ratio.

- 4 <sup>d</sup>Reacted guaiacol concentration (guaiacol was totally consumed in all experiments, so the reacted  
5 concentrations  $\Delta[\text{guaiacol}]$  correspond to  $[\text{guaiacol}]_0$ ).
- 6 <sup>e</sup>Organic aerosol mass concentration (corrected for wall losses and assuming a particle density of 1.4).
- 7 <sup>d</sup>Overall SOA yield (Y) calculated as the ratio of  $M_0$  to the total reacted guaiacol concentration.
- 8 <sup>e</sup>Initial  $\text{NO}_2$  volume ratio measured in the chamber (chemiluminescence  $\text{NO}_x$  analyser).
- 9 <sup>f</sup>Initial  $\text{O}_3$  volume ratio measured in the chamber (photometric  $\text{O}_3$  analyser).
- 10 <sup>g</sup>Initial injected  $\text{NO}_2$  volume ratio.
- 11 <sup>h</sup>Initial injected  $\text{O}_3$  volume ratio.
- 12

13 **Table 2.** Major compounds observed in the SOAs (ESI-LC-QToF-MS/MS analyses) formed  
 14 from the gas-phase reaction of guaiacol (2-methoxyphenol) with NO<sub>3</sub> radicals. The main  
 15 fragments obtained by MS/MS analyses (see Fig. S1-S8 in supporting information) and the  
 16 relative abundances (R, in %) are also indicated.

Molecular ion <sup>a</sup>	Main fragments	Brut Formula	Name <sup>e</sup>	Structure <sup>f</sup>	R (%) <sup>g</sup>
152	46 [NO <sub>2</sub> ] <sup>-</sup> 93 [C <sub>6</sub> H <sub>5</sub> O] <sup>-</sup> 122 [C <sub>7</sub> H <sub>6</sub> O <sub>2</sub> ] <sup>-</sup>	C <sub>7</sub> H <sub>6</sub> NO <sub>3</sub> <sup>d</sup>	Nitromethoxybenzene <sup>2</sup>		9.3
154	69 [C <sub>3</sub> HO <sub>2</sub> ] <sup>-</sup> 95 [C <sub>5</sub> H <sub>3</sub> O <sub>2</sub> ] <sup>-</sup> 123 [C <sub>6</sub> H <sub>3</sub> O <sub>3</sub> ] <sup>-</sup>	C <sub>6</sub> H <sub>4</sub> NO <sub>4</sub> <sup>d</sup>	Nitrocatechol <sup>1-2</sup>		18.0
168	95 [C <sub>5</sub> H <sub>3</sub> O <sub>2</sub> ] <sup>-</sup> 123 [C <sub>6</sub> H <sub>3</sub> O <sub>3</sub> ] <sup>-</sup> 153 [C <sub>6</sub> H <sub>3</sub> NO <sub>4</sub> ] <sup>-</sup>	C <sub>7</sub> H <sub>6</sub> NO <sub>4</sub> <sup>b</sup>	Nitroguaiacol <sup>4</sup>		11.7
197	76 [C <sub>5</sub> H <sub>2</sub> N] <sup>-</sup> 109 [CH <sub>5</sub> N <sub>2</sub> O <sub>4</sub> ] <sup>-</sup> 123 [C <sub>6</sub> H <sub>5</sub> NO <sub>2</sub> ] <sup>-</sup>	C <sub>7</sub> H <sub>5</sub> N <sub>2</sub> O <sub>5</sub> <sup>c</sup>	Dinitromethoxybenzene <sup>2</sup>		7.6
199	67 [C <sub>4</sub> H <sub>3</sub> O] <sup>-</sup> 95 [C <sub>5</sub> H <sub>3</sub> O <sub>2</sub> ] <sup>-</sup> 153 [C <sub>6</sub> H <sub>3</sub> NO <sub>4</sub> ] <sup>-</sup>	C <sub>6</sub> H <sub>3</sub> N <sub>2</sub> O <sub>6</sub> <sup>b</sup>	Dinitrocatechol <sup>3</sup>		4.7
213	66 [C <sub>3</sub> NO] <sup>-</sup> 78 [C <sub>5</sub> H <sub>2</sub> O] <sup>-</sup> 198 [C <sub>6</sub> H <sub>2</sub> N <sub>2</sub> O <sub>6</sub> ] <sup>-</sup>	C <sub>7</sub> H <sub>5</sub> N <sub>2</sub> O <sub>6</sub> <sup>b</sup>	Dinitroguaiacol <sup>6</sup>		9.0
321	153 [C <sub>6</sub> H <sub>3</sub> NO <sub>4</sub> ] <sup>-</sup> 168 [C <sub>7</sub> H <sub>6</sub> NO <sub>4</sub> ] <sup>-</sup> 306 [C <sub>12</sub> H <sub>6</sub> N <sub>2</sub> O <sub>8</sub> ] <sup>-</sup>	C <sub>13</sub> H <sub>9</sub> N <sub>2</sub> O <sub>8</sub> <sup>b</sup>	Association of 1 nitroguaiacol and 1 nitrocatechol <sup>12</sup>		5.4
335	153 [C <sub>6</sub> H <sub>3</sub> NO <sub>4</sub> ] <sup>-</sup> 168 [C <sub>7</sub> H <sub>6</sub> NO <sub>4</sub> ] <sup>-</sup> 320 [C <sub>16</sub> H <sub>6</sub> N <sub>3</sub> O <sub>5</sub> ] <sup>-</sup>	C <sub>14</sub> H <sub>11</sub> N <sub>2</sub> O <sub>8</sub> <sup>b</sup>	Association of 2 nitroguaiacols <sup>5</sup>		18.1

531	-	-	-	-	8.2
587	-	-	-	-	4.3

18 <sup>a</sup>The indicated masses correspond to the [M–H] product ions.

19 <sup>b</sup>Probability given by the software between 98 and 100 %.

20 <sup>c</sup>Probability given by the software between 90 and 97 %.

21 <sup>d</sup>Probability given by the software between 70 and 89%.

22 <sup>e</sup>Number of detected isomers.

23 <sup>f</sup>The drawn structure correspond to one isomer only.

24 <sup>g</sup>The relative abundances (in %) were calculated from the ratio of the sum of the chromatographic

25 areas of the different isomers to the total chromatographic area of all the peaks.